

Numerical Simulation of Microflows with Moment Method

Zhenning CAI^{1,*}

* Corresponding author: Tel.: ++44 (0)1575 6378931; Email: cai@mathcces.rwth-aachen.de
1 Center for Computational Engineering Science, RWTH Aachen University, Germany

Abstract A series of hyperbolic moment equations is derived for the Boltzmann equation with ES-BGK collision term. These systems can be obtained through a slight modification in the deduction of Grad's moment equations, and such a method is suitable for deriving systems with moments up to any order. The systems are equipped with proper wall boundary conditions so that the number of equations in the boundary conditions is consistent with the hyperbolic structure of the moment system. Our numerical scheme for solving the hyperbolic moment systems is of second order, and a special mapping method is introduced so that the numerical efficiency is highly enhanced. Our numerical results are validated by comparison with the DSMC results. Through the numerical solutions of systems with increasing number of moments, the convergence of the moment method is clearly observed.

Keywords: Micro Flow, Moment Equations, Boundary Condition, Finite Volume Method

1. Introduction

In the field of microflows, traditional gas models such as the Euler equations and the Navier-Stokes equations can hardly predict the flow states accurately when the flow is in the transitional regime. An important way to construct extended models is the moment method. The moment method was proposed by Grad (1949), and his thirteen-moment theory is a first application beyond the classical hydrodynamics. The 13-moment method was later improved by regularizations based on the Chapman-Enskog expansion or the method of "order of magnitudes" (Struchtrup and Torrilhon, 2003; Struchtrup, 2005), and some numerical test of the regularized 13-moment equations already show its potential use in the field of microflows (Torrilhon, 2006; Rana et al., 2013). Meanwhile, moment systems with large number of moments are also investigated. In such cases, the moment method can also be considered as an efficient way to discretize the Boltzmann equation. However, during a long time, two major obstacles strongly retard the development in this direction: one is the loss of global hyperbolicity, and the other is the difficulty in constructing boundary conditions, which is crucial in the microflow simulations.

Recently, some progress is made (Cai et al., 2013b; Cai et al., 2014a) and we are going to carry out some simplest applications in this paper.

The present paper adopts the hyperbolic moment models proposed in the work of Cai et al. (2014a), where a series of globally hyperbolic moment models are presented. The global hyperbolicity enables robust numerical simulation with the moment method. In this paper, these models are reviewed and more insights of them are revealed through rational derivation of these models from the Boltzmann equation. The wall boundary conditions for this set of moment systems are already derived by Cai et al. (2013b), and in this paper, they are restructured for easier understanding. The numerical method is based on the scheme presented by Cai et al. (2013b). Here we extend it to a second-order scheme so that the numerical efficiency is highly enhanced. Two numerical examples are carried out to show the accuracy and convergence of the moment method. Comparing with former similar works (Cai et al., 2012; Cai et al., 2013b), both the advanced models and the advanced numerical techniques are integrated in this work.

Below, the Boltzmann equation and the ES-BGK model are reviewed in Section 2. The

derivation of the hyperbolic moment systems and the boundary conditions are presented respectively in Section 3 and Section 4. Section 5 briefly introduces the numerical method and the numerical results are carried out in Section 6. Finally, some concluding remarks are made in Section 7.

2. Boltzmann equation and the ES-BGK model

Boltzmann equation is the fundamental model in the gas kinetic theory. It reads

$$\frac{\partial f}{\partial t} + \mathbf{c} \cdot \nabla_{\mathbf{x}} f + \mathbf{F} \cdot \nabla_{\mathbf{c}} f = Q(f, f)$$

$$t \in \mathbb{R}^+, \quad \mathbf{x} = (x_1, x_2, x_3)^T \in \mathbb{R}^3, \quad (1)$$

$$\mathbf{c} = (c_1, c_2, c_3)^T \in \mathbb{R}^3,$$

where $f(t, \mathbf{x}, \mathbf{c})$ is the distribution function, and $t, \mathbf{x}, \mathbf{c}$ stand for the time, the spatial coordinate and the velocity of gas molecules respectively. The distribution function provides a statistical view of the motion of particles, and macroscopic quantities such as the density ρ , the velocity \mathbf{u} and the pressure p can be obtained through integration on the distribution function:

$$\rho(t, \mathbf{x}) = m \int_{\mathbb{R}^3} f(t, \mathbf{x}, \mathbf{c}) \, d\mathbf{c},$$

$$\mathbf{u}(t, \mathbf{x}) = \frac{m}{\rho(t, \mathbf{x})} \int_{\mathbb{R}^3} \mathbf{c} f(t, \mathbf{x}, \mathbf{c}) \, d\mathbf{c}, \quad (2)$$

$$p(t, \mathbf{x}) = \frac{m}{3} \int_{\mathbb{R}^3} \|\mathbf{c} - \mathbf{u}\|^2 f(t, \mathbf{x}, \mathbf{c}) \, d\mathbf{c},$$

where m is the mass of a single gas molecule.

In equation (1), the vector \mathbf{F} is an external force which accelerates the gas molecules. The right hand side $Q(f, f)$ is the collision term demonstrating the interaction between particles. The collision term $Q(f, f)$ has a quadratic form with a five-dimensional integral, which is inconvenient for the numerical implementation. As a simplification, we replace it by an approximation, which is called the ellipsoidal-statistical Bhatnagar-Gross-Krook (ES-BGK) operator proposed by Holway (1966):

$$Q_{\text{ES-BGK}}(f) = \frac{\text{Pr}}{\tau} (f^{\text{ES}} - f), \quad (3)$$

where Pr is the Prandtl number of the gas, τ is the relaxation time, and f^{ES} is the quasi-equilibrium defined by

$$f^{\text{ES}} = \frac{\rho/m}{\sqrt{\det(2\pi\Lambda)}} \exp\left(-\frac{\mathbf{C}^T \Lambda^{-1} \mathbf{C}}{2}\right). \quad (4)$$

In (4), \mathbf{C} is the relative velocity defined by $\mathbf{C} = \mathbf{c} - \mathbf{u}$. The matrix $\Lambda = (\lambda_{ij})$ is a 3×3 matrix with

$$\lambda_{ij} = \frac{p\delta_{ij} + (1 - 1/\text{Pr})\sigma_{ij}}{\rho}, \quad i, j = 1, 2, 3,$$

where δ_{ij} is the Kronecker symbol, and σ_{ij} is the stress tensor:

$$\sigma_{ij}(t, \mathbf{x}) = \int_{\mathbb{R}^3} C_i C_j f(t, \mathbf{x}, \mathbf{c}) \, d\mathbf{c} - \delta_{ij} p(t, \mathbf{x}). \quad (5)$$

Compared with the classical BGK model (which uses $\Lambda = p\mathbf{I}$ in (4)), the ES-BGK model provides correct Prandtl number for the gas flows.

3. Hyperbolic Moment Equations

3.1 The infinite moment system

Solving the Boltzmann equation directly is quite a challenging task, since the distribution function is a seven-dimensional function. Additionally, the domain of the velocity variable \mathbf{c} is always an unbounded domain \mathbb{R}^3 , even if the gas is confined in a closed containment. In order to discretize the velocity variable efficiently, Grad (1949) proposed to expand the distribution function into the following series:

$$f(t, \mathbf{x}, \mathbf{c}) = \sum_{\alpha \in \mathbb{N}^3} f_{\alpha}(t, \mathbf{x}) \mathcal{H}_{\alpha}^{[\theta(t, \mathbf{x})]} \left(\frac{\mathbf{c} - \mathbf{u}(t, \mathbf{x})}{\sqrt{\theta(t, \mathbf{x})}} \right), \quad (6)$$

where α is a 3D multi-index, and the basis functions are defined by

$$\mathcal{H}_{\alpha}^{[\theta]}(\mathbf{v}) = \frac{\theta^{-(\alpha_1 + \alpha_2 + \alpha_3)/2}}{m(2\pi\theta)^{3/2}} \prod_{k=1}^3 He_{\alpha_k}(v_k) \exp\left(-\frac{v_k^2}{2}\right),$$

$$\forall \alpha = (\alpha_1, \alpha_2, \alpha_3) \in \mathbb{N}^3, \quad \mathbf{v} = (v_1, v_2, v_3)^T \in \mathbb{R}^3.$$

In the above equation, $He_n(x)$ is the Hermite polynomial of degree n , defined by

$$He_n(x) = (-1)^n \exp(x^2/2) \frac{d^n}{dx^n} \exp(-x^2/2),$$

and θ is the scaled temperature defined by $\theta(t, \mathbf{x}) = p(t, \mathbf{x})/\rho(t, \mathbf{x})$. Substituting the

expansion (6) into (2) and (5), one has

$$f_0 = \rho, \quad f_{e_j} = 0, \quad j = 1, 2, 3,$$

$$f_{e_i+e_j} = (1 + \delta_{ij})^{-1} \sigma_{ij}, \quad i, j = 1, 2, 3.$$

The governing equations of the coefficients $f_{\mathbf{a}}(t, \mathbf{x})$ is obtained by substituting the expansion (6) into the Boltzmann equation:

$$\begin{aligned} \frac{\partial f_{\mathbf{a}}}{\partial t} + \sum_{k=1}^3 \left(\frac{\partial u_k}{\partial t} - F_k \right) f_{\mathbf{a}-\mathbf{e}_k} + \frac{1}{2} \frac{\partial \theta}{\partial t} \sum_{k=1}^3 f_{\mathbf{a}-2\mathbf{e}_k} + \\ \sum_{j=1}^3 \left(\theta \frac{\partial f_{\mathbf{a}-\mathbf{e}_j}}{\partial x_j} + u_j \frac{\partial f_{\mathbf{a}}}{\partial x_j} + (\alpha_j + 1) \frac{\partial f_{\mathbf{a}+\mathbf{e}_j}}{\partial x_j} \right) + \\ \sum_{j,k=1}^3 \frac{\partial u_k}{\partial x_j} \left(\theta f_{\mathbf{a}-\mathbf{e}_j-\mathbf{e}_k} + u_j f_{\mathbf{a}-\mathbf{e}_k} + (\alpha_j + 1) f_{\mathbf{a}+\mathbf{e}_j-\mathbf{e}_k} \right) + \\ \frac{1}{2} \sum_{j,k=1}^3 \frac{\partial \theta}{\partial x_j} \left(\theta f_{\mathbf{a}-\mathbf{e}_j-2\mathbf{e}_k} + u_j f_{\mathbf{a}-2\mathbf{e}_k} + (\alpha_j + 1) f_{\mathbf{a}+\mathbf{e}_j-2\mathbf{e}_k} \right) \\ = P_{\mathbf{a}}, \quad \forall \mathbf{a} \in \mathbb{N}^3, \end{aligned}$$

where $P_{\mathbf{a}}$ is the corresponding collision term, and f_{β} is taken as zero if any component of the subscript β is negative. For simplicity, the above system is abbreviated as

$$\mathcal{L}_{\mathbf{a}} = P_{\mathbf{a}}, \quad \forall \mathbf{a} \in \mathbb{N}^3. \quad (7)$$

For the ES-BGK model,

$$P_{\mathbf{a}} = \frac{\text{Pr}}{\tau} (f_{\mathbf{a}}^{\text{ES}} - f_{\mathbf{a}}),$$

$$f_{\mathbf{a}}^{\text{ES}} =$$

$$\begin{cases} \rho, & \mathbf{a} = \mathbf{0}, \\ 0, & |\mathbf{a}| = 1, \\ \frac{1 - \text{Pr}}{\alpha_i \rho} \sum_{j=1}^3 \sigma_{ij} f_{\mathbf{a}-\mathbf{e}_i-\mathbf{e}_j}^{\text{ES}}, & |\mathbf{a}| \geq 2 \text{ and } \alpha_i > 0. \end{cases}$$

Note that $f_{\mathbf{a}}^{\text{ES}}$ is given recursively, and the recursion (the last case in the expression of $f_{\mathbf{a}}^{\text{ES}}$) holds as long as the i th component of \mathbf{a} is positive. For example, if $\mathbf{a} = (3, 5, 0)$, both of the following two relations are correct:

$$f_{\mathbf{a}}^{\text{ES}} = \frac{1 - 1/\text{Pr}}{3\rho} \sum_{j=1}^3 \sigma_{1j} f_{\mathbf{a}-\mathbf{e}_1-\mathbf{e}_j}^{\text{ES}},$$

$$f_{\mathbf{a}}^{\text{ES}} = \frac{1 - 1/\text{Pr}}{5\rho} \sum_{j=1}^3 \sigma_{2j} f_{\mathbf{a}-\mathbf{e}_2-\mathbf{e}_j}^{\text{ES}}.$$

The system (7) contains infinite number of equations, and each equation is a ‘‘moment equation’’.

3.2 Derivation of hyperbolic moment systems

A practical model allows containing only finite number of equations. However, any finite subset of (7) contains at least one coefficient whose evolution cannot be described by this subset. Thus the ‘‘moment closure’’ is needed. A simple way is to set all the coefficients $f_{\mathbf{a}}$ with $|\mathbf{a}| > M$ to be zero for some positive integer $M \geq 2$, which is called ‘‘Grad’s moment method’’. However, it has been shown by Cai et al. (2013a) that in the one-dimensional case, when $M > 2$, the resulting moment system is only hyperbolic around the equilibrium state ($f_{\mathbf{a}} = 0$ for all $\mathbf{a} \neq \mathbf{0}$). Since the hyperbolicity directly affects the existence of the solution for a first-order quasi-linear partial differential system, the application of Grad’s moment method is strongly limited due to such a deficiency.

In the paper of Cai et al. (2014a), the authors proposed a series of globally hyperbolic moment systems by a slight modification on the original Grad’s moment method. However, it is never mentioned how these systems are derived, and the reason of their global hyperbolicity becomes mysterious. The underlying mechanism is not revealed until recently. Due to the limit of the paper length, only the main idea is presented.

Below, a direct derivation of hyperbolic moment equations from the Boltzmann equation is presented. It contains the following six steps:

- (1) Select a positive integer $M \geq 2$ so that the resulting moment system will contain only $f_{\mathbf{a}}$ with $|\mathbf{a}| \leq M$.
- (2) Approximate the distribution function f by

$$f \approx \tilde{f} = \sum_{|\mathbf{a}| \leq M} f_{\mathbf{a}} \mathcal{H}_{\mathbf{a}}^{[\theta]} \left(\frac{\mathbf{c} - \mathbf{u}}{\sqrt{\theta}} \right). \quad (8)$$

- (3) Expand the derivatives of \tilde{f} and the collision term into series:

$$\begin{aligned} \frac{\partial \tilde{f}}{\partial t} &= \sum_{\mathbf{a} \in \mathbb{N}^3} f_{\mathbf{a}} \mathcal{H}_{\mathbf{a}}^{[\theta]}, & \nabla_{\mathbf{x}} \tilde{f} &= \sum_{\mathbf{a} \in \mathbb{N}^3} \mathbf{G}_{\mathbf{a}} \mathcal{H}_{\mathbf{a}}^{[\theta]}, \\ \nabla_{\mathbf{c}} \tilde{f} &= \sum_{\mathbf{a} \in \mathbb{N}^3} \mathbf{H}_{\mathbf{a}} \mathcal{H}_{\mathbf{a}}^{[\theta]}, & Q(\tilde{f}) &= \sum_{\mathbf{a} \in \mathbb{N}^3} P_{\mathbf{a}} \mathcal{H}_{\mathbf{a}}^{[\theta]}, \end{aligned}$$

where we omit the parameter of the function $\mathcal{H}_a^{[\theta]}$ (which should be $(\mathbf{c}-\mathbf{u})/\sqrt{\theta}$) for conciseness. Note that F_a and \mathbf{G}_a contain derivative operators, while \mathbf{H}_a and P_a do not.

(4) Truncate in these expansions:

$$\begin{aligned}\frac{\partial \tilde{f}}{\partial t} &\approx \sum_{|\mathbf{a}| \leq M} F_a \mathcal{H}_a^{[\theta]}, & \nabla_{\mathbf{x}} \tilde{f} &\approx \sum_{|\mathbf{a}| \leq M} \mathbf{G}_a \mathcal{H}_a^{[\theta]}, \\ \nabla_{\mathbf{c}} \tilde{f} &\approx \sum_{|\mathbf{a}| \leq M} \mathbf{H}_a \mathcal{H}_a^{[\theta]}, & Q(\tilde{f}) &\approx \sum_{|\mathbf{a}| \leq M} P_a \mathcal{H}_a^{[\theta]}.\end{aligned}$$

(5) Based on the approximation of $\nabla_{\mathbf{x}} \tilde{f}$, calculate the convection term $\mathbf{c} \cdot \nabla_{\mathbf{x}} \tilde{f}$ and truncate the result:

$$\begin{aligned}\mathbf{c} \cdot \nabla_{\mathbf{x}} \tilde{f} &\approx \mathbf{c} \cdot \sum_{|\mathbf{a}| \leq M} \mathbf{G}_a \mathcal{H}_a^{[\theta]} = \sum_{\mathbf{a} \in \mathbb{N}^3} G_a \mathcal{H}_a^{[\theta]} \\ &\approx \sum_{|\mathbf{a}| \leq M} G_a \mathcal{H}_a^{[\theta]}.\end{aligned}$$

(6) Substitute the above approximations into the Boltzmann equation, and the result

$$\begin{aligned}F_a + G_a + \mathbf{F} \cdot \mathbf{H}_a &= P_a, \\ \forall \mathbf{a} \in \mathbb{N}^3, & |\mathbf{a}| \leq M\end{aligned}\quad (9)$$

is the hyperbolic moment system.

In the above procedure, all the coefficients F_a, G_a, \mathbf{H}_a can be written as combinations of f_a, \mathbf{u}, θ and their derivatives. We comment here that the above procedure is very similar as the derivation of Grad's moment systems, and the only difference is that in the fourth step, Grad's moment method does not apply the truncation to the spatial derivative term. The unequal process of the time derivative and the spatial derivative leads to the loss of global hyperbolicity. Comparing with the discrete velocity model, the moment system is rotationally invariant, which means the same number of degrees of freedom is used to discretize the velocity space in all directions. Thus, consider a discrete velocity method using $(M+1) \times (M+1) \times (M+1)$ discrete velocities and a moment method expanding the distribution function up to polynomials of degree M . The former has $(M+1)^3$ degrees of freedom, and the latter has only $(M+1)(M+2)(M+3)/6$ degrees of freedom. Below we give the final expression of the

hyperbolic moment system (9):

$$\begin{aligned}\frac{\partial f_{\mathbf{a}}}{\partial t} + \sum_{k=1}^3 \left(\frac{\partial u_k}{\partial t} - F_k \right) f_{\mathbf{a}-\mathbf{e}_k} + \frac{1}{2} \frac{\partial \theta}{\partial t} \sum_{k=1}^3 f_{\mathbf{a}-2\mathbf{e}_k} + \\ \sum_{j=1}^3 \left(\theta \frac{\partial f_{\mathbf{a}-\mathbf{e}_j}}{\partial x_j} + u_j \frac{\partial f_{\mathbf{a}}}{\partial x_j} + \kappa_{j,\mathbf{a},M} \frac{\partial f_{\mathbf{a}+\mathbf{e}_j}}{\partial x_j} \right) + \\ \sum_{j,k=1}^3 \frac{\partial u_k}{\partial x_j} \left(\theta f_{\mathbf{a}-\mathbf{e}_j-\mathbf{e}_k} + u_j f_{\mathbf{a}-\mathbf{e}_k} + \kappa_{j,\mathbf{a},M} f_{\mathbf{a}+\mathbf{e}_j-\mathbf{e}_k} \right) + \\ \frac{1}{2} \sum_{j,k=1}^3 \frac{\partial \theta}{\partial x_j} \left(\theta f_{\mathbf{a}-\mathbf{e}_j-2\mathbf{e}_k} + u_j f_{\mathbf{a}-2\mathbf{e}_k} + \kappa_{j,\mathbf{a},M} f_{\mathbf{a}+\mathbf{e}_j-2\mathbf{e}_k} \right) \\ = P_{\mathbf{a}}, \quad \forall \mathbf{a} \in \mathbb{N}^3, \quad |\mathbf{a}| \leq M,\end{aligned}$$

where

$$\kappa_{j,\mathbf{a},M} = \begin{cases} 0, & |\mathbf{a}| = M, \\ \alpha_j + 1, & |\mathbf{a}| < M. \end{cases}$$

4. Boundary Conditions

The wall boundary conditions are important in the simulation of microflows. For the Boltzmann equation, a popular choice is Maxwell's boundary condition (Maxwell, 1878):

$$\begin{aligned}f(t, \mathbf{x}, \mathbf{c}) &= \chi f_M^W(t, \mathbf{x}, \mathbf{c}) + (1-\chi) f(t, \mathbf{x}, \mathbf{c}'), \\ &\text{for } (\mathbf{c}-\mathbf{u}^W) \cdot \mathbf{n} < 0,\end{aligned}$$

where \mathbf{n}, \mathbf{u}^W and χ are respectively the outer normal vector, the velocity and the accommodation coefficient of the wall, and f_M^W and \mathbf{c}' are defined by

$$f_M^W(t, \mathbf{x}, \mathbf{c}) = \frac{\rho^W}{(2\pi\theta^W)^{3/2}} \exp\left(-\frac{\|\mathbf{c}-\mathbf{u}^W\|^2}{2\theta^W}\right),$$

$$\mathbf{c}' = \mathbf{c} - 2(\mathbf{C}^W \cdot \mathbf{n})\mathbf{n}, \quad \mathbf{C}^W \triangleq \mathbf{c} - \mathbf{u}^W.$$

Here θ^W is the temperature of the wall, and ρ^W is determined by the condition that the mass flux on the boundary should be zero:

$$\int_{\mathbf{C}^W \cdot \mathbf{n} < 0} (\mathbf{C}^W \cdot \mathbf{n}) [f_M^W(t, \mathbf{x}, \mathbf{c}) - f(t, \mathbf{x}, \mathbf{c}')] d\mathbf{c} = 0.$$

From the above relations, it is not difficult to obtain $\mathbf{u}^W \cdot \mathbf{n} = \mathbf{u} \cdot \mathbf{n}$. Following Torrilhon (2014), we define

$$f^{(\text{odd})}(\mathbf{c}) = \frac{f(\mathbf{c}) - f(\mathbf{c}')}{2}, \quad f^{(\text{even})}(\mathbf{c}) = \frac{f(\mathbf{c}) + f(\mathbf{c}')}{2},$$

and thus the boundary condition can be rewritten as

$$f^{(\text{odd})} = \frac{\chi}{2-\chi}(f_M^W - f^{(\text{even})}), \text{ for } \mathbf{C}^W \cdot \mathbf{n} < 0. \quad (10)$$

The boundary conditions of moment systems are deduced based on the form (10). For conciseness, we assume $\mathbf{n} = (1, 0, 0)^T$. Thus $u_1^W = u_1$ and we have the following expansion of $f^{(\text{odd})}$ and $f^{(\text{even})}$:

$$\begin{aligned} f^{(\text{odd})} &= \sum_{\alpha \in \mathbb{N}^3, \alpha_1 \text{ is odd}} f_\alpha \mathcal{H}_\alpha^{[\theta]} \left(\frac{\mathbf{c} - \mathbf{u}}{\sqrt{\theta}} \right), \\ f^{(\text{even})} &= \sum_{\alpha \in \mathbb{N}^3, \alpha_1 \text{ is even}} f_\alpha \mathcal{H}_\alpha^{[\theta]} \left(\frac{\mathbf{c} - \mathbf{u}}{\sqrt{\theta}} \right). \end{aligned} \quad (11)$$

According to Grad (1949), the boundary conditions of the moment equations should contain only the moments of (10) which are odd in the direction of \mathbf{n} . Define

$$\mathcal{E}\psi(\mathbf{c}) = \begin{cases} 0, & \mathbf{C}^W \cdot \mathbf{n} > 0, \\ \psi(\mathbf{c}), & \mathbf{C}^W \cdot \mathbf{n} < 0. \end{cases}$$

Then taking moments in (10) is equivalent to expanding $\mathcal{E}f^{\text{odd}}$ and $\mathcal{E}(f_M^W - f^{(\text{even})})$ into series. Precisely, if

$$\tilde{\mathcal{E}}f^{(\text{odd})} = \sum_{\alpha \in \mathbb{N}^3} \tilde{f}_\alpha^{(\text{odd})} \mathcal{H}_\alpha^{[\theta]} \left(\frac{\mathbf{c} - \mathbf{u}}{\sqrt{\theta}} \right),$$

$$\mathcal{E}(f_M^W - \tilde{f}^{(\text{even})}) = \sum_{\alpha \in \mathbb{N}^3} \tilde{f}_\alpha^{(W-\text{even})} \mathcal{H}_\alpha^{[\theta]} \left(\frac{\mathbf{c} - \mathbf{u}}{\sqrt{\theta}} \right),$$

where $\tilde{f}^{(\text{odd})}$ and $\tilde{f}^{(\text{even})}$ are respectively the odd and even parts of \tilde{f} (see (8) and (11)), then the boundary conditions of the moment equations are

$$\tilde{f}_\alpha^{(\text{odd})} = \frac{\chi}{2-\chi} \tilde{f}_\alpha^{(W-\text{even})}, \quad |\alpha| \leq M \text{ and } \alpha_1 \text{ is odd.}$$

When α_1 is odd, it can be discovered from (11) that $\tilde{f}_\alpha^{(\text{odd})} = f_\alpha / 2$, and $\tilde{f}_\alpha^{(W-\text{even})}$ is a function of $\mathbf{u}, \mathbf{u}^W, \theta, \theta^W$ and f_β with even β_1 . Thus the boundary conditions can be written clearer as

$$\begin{aligned} f_\alpha &= \frac{2\chi}{2-\chi} B_\alpha(\mathbf{u}, \mathbf{u}^W, \theta, \theta^W; f_\beta |_{|\beta| \leq M} \text{ and } \beta_1 \text{ is even}), \\ & \quad |\alpha| \leq M \text{ and } \alpha_1 \text{ is odd.} \end{aligned}$$

The detailed expression and derivation of B_α can be found in the paper of Cai et al. (2012). The above boundary conditions fit the

hyperbolic moment system very well. It has been proved by Cai et al. (2013b) that the number of equations in the boundary condition exactly equals what is required by the hyperbolicity.

5. Numerical Method

The numerical method in our simulation is an improved version of the one presented by Cai et al. (2013b). We first rewrite the moment system in the following abstract form:

$$\frac{\partial \mathbf{q}}{\partial t} + \sum_{k=1}^3 \left[\frac{\partial \mathbf{F}_k(\mathbf{q})}{\partial x_k} + \mathbf{A}_k(\mathbf{q}) \frac{\partial \mathbf{q}}{\partial x_k} \right] = \mathbf{P}(\mathbf{q}), \quad (12)$$

where \mathbf{q} is the vector of unknowns, and the conservative part $\partial_t \mathbf{q} + \sum_{k=1}^3 \partial_{x_k} \mathbf{F}_k(\mathbf{q}) = \mathbf{P}(\mathbf{q})$ is the corresponding moment system of Grad-type. As in the reference paper (Cai et al., 2013b), we split (12) into two equations

$$\frac{\partial \mathbf{q}}{\partial t} + \sum_{k=1}^3 \left[\frac{\partial \mathbf{F}_k(\mathbf{q})}{\partial x_k} + \mathbf{A}_k(\mathbf{q}) \frac{\partial \mathbf{q}}{\partial x_k} \right] = 0 \quad (13)$$

and

$$\frac{\partial \mathbf{q}}{\partial t} = \mathbf{P}(\mathbf{q}), \quad (14)$$

and apply Strang's method as follows:

- (1) Given an initial value $\mathbf{q}(t_n) = \mathbf{q}^n$, evolve \mathbf{q}^n according to (14) by a half time step $(\Delta t/2)$. The result is denoted by \mathbf{q}^{n*} .
- (2) Evolve \mathbf{q}^{n*} by a full time step Δt according to (13). The result is denoted by \mathbf{q}^{n**} .
- (3) Evolve \mathbf{q}^{n**} by a half time step $(\Delta t/2)$ according to (14). The result is an approximation to $\mathbf{q}(t_n + \Delta t)$.

Strang's method is second order in t .

In the first and third steps, the system (14) is solved analytically. Through the expression of the hyperbolic moment systems, it can be found that the system (14) is equivalent to

$$\begin{aligned} \frac{\partial f_\alpha}{\partial t} + \sum_{k=1}^3 \left(\frac{\partial u_k}{\partial t} - F_k \right) f_{\alpha - \mathbf{e}_k} + \frac{1}{2} \frac{\partial \theta}{\partial t} \sum_{k=1}^3 f_{\alpha - 2\mathbf{e}_k} &= P_\alpha, \\ \forall \alpha \in \mathbb{N}^3, \quad |\alpha| \leq M. \end{aligned}$$

The exact solutions are

$$\mathbf{u}(t + \Delta t) = \mathbf{u}(t) + \Delta t \cdot \mathbf{F}, \quad \theta(t + \Delta t) = \theta(t),$$

$$f_a(t + \Delta t) = \left[f_a(t) - \frac{\text{Pr}}{\text{Pr} - \frac{1}{2}|\boldsymbol{\alpha}|} K_a(t) \right] \exp\left(-\frac{\text{Pr}}{\tau} t\right) + \frac{\text{Pr}}{\text{Pr} - \frac{1}{2}|\boldsymbol{\alpha}|} K_a(t) \exp\left(-\frac{|\boldsymbol{\alpha}|}{2} \cdot \frac{t}{\tau}\right),$$

where $K_a(t)$ is defined recursively as

$$K_a(t) = \begin{cases} \rho(t), & \boldsymbol{\alpha} = \mathbf{0}; \\ \frac{1 - \text{Pr}}{\alpha_i \rho(t)} \sum_{j=1}^3 \sigma_{ij}(t) K_{a-e_i-e_j}(t), & |\boldsymbol{\alpha}| \geq 2, \alpha_i > 0 \text{ and } |\boldsymbol{\alpha}| \text{ is even;} \\ 0, & |\boldsymbol{\alpha}| \text{ is odd.} \end{cases}$$

Now we focus on the numerical solution of (13). In (13), the non-conservative product $\mathbf{A}_k(\mathbf{q}) \partial_{x_k} \mathbf{q}$ is interpreted by the DLM theory (Dal Maso et al., 1995), which requires a cluster of paths $\Phi(s; \mathbf{q}_1, \mathbf{q}_2)$ to be defined so that the shock condition can be determined. The choice of the paths is not crucial in this paper, and we simply use

$$\Phi(s; \mathbf{q}_1, \mathbf{q}_2) = (1-s)\mathbf{q}_1 + s\mathbf{q}_2, \quad s \in [0, 1]$$

in our implementation.

In this paper, we consider only the case that the distribution function varies only in the x_1 direction, and a uniform grid is used for spatial discretization. The numerical scheme of (13) is a finite volume method with a non-conservative version of the HLL numerical flux. The semi-discrete system is

$$\frac{d\mathbf{q}_j}{dt} = -\frac{\hat{\mathbf{F}}_{j+1/2} - \hat{\mathbf{F}}_{j-1/2}}{\Delta x} - \frac{\hat{\mathbf{G}}_{j+1/2}^- - \hat{\mathbf{G}}_{j-1/2}^+}{\Delta x} - \mathbf{A}_1(\mathbf{q}_j) \frac{\mathbf{q}_{j+1/2}^- - \mathbf{q}_{j-1/2}^+}{\Delta x}, \quad (15)$$

where we use a linear reconstruction with the monotonized central (MC) limiter to achieve the high resolution, and $\mathbf{q}_{j+1/2}^\pm$ stands for the left (-) and right (+) limit of the reconstructed solution at the grid point $x_{j+1/2}$. In (15), the conservative numerical fluxes $\hat{\mathbf{F}}_{j\pm 1/2}$ are the normal HLL fluxes for the conservative part $\partial_x \mathbf{F}_1(\mathbf{q})$, and we omit their expressions here. The non-conservative numerical fluxes are

$$\hat{\mathbf{G}}_{j+1/2}^\pm = \begin{cases} 0, & \lambda_{j+1/2}^\pm \leq 0, \\ \frac{\lambda_{j+1/2}^\pm}{\lambda_{j+1/2}^- - \lambda_{j+1/2}^+} \mathbf{g}_{j+1/2}, & \lambda_{j+1/2}^- \leq 0 \leq \lambda_{j+1/2}^+, \\ \mp \mathbf{g}_{j+1/2}, & \lambda_{j+1/2}^{mp} \geq 0, \end{cases}$$

where $\lambda_{j+1/2}^+$ ($\lambda_{j+1/2}^-$) is the maximum (minimum) value among the eigenvalues of $\partial_x \mathbf{F}_1(\mathbf{q}_j) + \mathbf{A}_1(\mathbf{q}_j)$ and $\partial_x \mathbf{F}_1(\mathbf{q}_{j+1}) + \mathbf{A}_1(\mathbf{q}_{j+1})$, and $\mathbf{g}_{j+1/2}$ is defined by

$$\mathbf{g}_{j+1/2} = \int_0^1 \mathbf{A}_1(\Phi(s; \mathbf{q}_{j+1/2}^-, \mathbf{q}_{j+1/2}^+)) \frac{\partial \Phi}{\partial s}(s; \mathbf{q}_{j+1/2}^-, \mathbf{q}_{j+1/2}^+) ds.$$

This numerical scheme is actually a finite volume version of the method proposed by Rhebergen et al. (2008). Finally, in order to keep the stability and retain the second order in the whole numerical scheme, the semi-discrete equation (15) is numerically solved by Heun's method.

Cai et al. (2013b) used a numerical skill to accelerate the evaluation of the conservative numerical flux $\hat{\mathbf{F}}_{j\pm 1/2}$. The central idea is to use different inertial frames of reference in different cells so that an approximate and fast mapping between the primitive moments and the conservative moments can be constructed numerically. This skill is originally proposed by Cai and Li (2010), and recently, an improved version of the mapping is introduced by Cai et al. (2014b) and is adopted in our numerical experiments. We refer the readers to the work of Cai et al. (2013b, 2014b) for details.

6. Numerical Examples

6.1 Heat transfer between parallel plates

The heat transfer between infinite parallel plates is one of the most fundamental processes in the field of microflows. Here we adopt the settings considered by Wadsworth D. C. (1993), where the gas is helium and the temperatures of the plates are 0.2894 and 1.0769 (nondimensionalized). For helium, the relaxation time based on the variable hard sphere model is

$$\tau = \sqrt{\frac{\pi}{2}} \frac{15Kn}{(5-2\omega)(7-2\omega)} \frac{\theta^{\omega-1}}{\rho}, \quad (16)$$

where the viscosity index ω is 0.657, and Kn is the ratio of the mean free path of the gas in free stream to the distance between the plates. In our simulation, we set the distance between the plates to be 1.0, and both plates have the same accommodation coefficient 0.58.

Since the definitions of the Knudsen number in Wadsworth's paper and this paper are slightly different, we choose $Kn = 0.0658, 0.1044$ and 0.3521 to match the settings of Wadsworth D. C. (1993). The numerical results are shown in Figs. 1-3, where the density is normalized by the center line value, and the temperature is normalized by the temperature of the left plate. Due to the flexibility in the number of moments, we use different M for different Knudsen numbers. For $Kn = 0.0658$, $M = 8$ is enough to get a good result, and for $Kn = 0.1044$ and 0.3521 , we use $M = 10$ and $M = 14$ respectively. Both the DSMC results and the experiment results are presented as references. Perfect agreement is found between our results and the DSMC results. The same problem is considered also by Cai, et al. (2013b), while the authors used 2000 grids for spatial discretization, and only 200 grids are used in this paper. The results are equally good.

6.2 Force-driven Poiseuille flow

Here we consider the force-driven Poiseuille flow which was simulated with the DSMC method by Zheng et al. (2002). In a non-dimensionalized setting, the temperatures of both walls are set to be 1, and the external force parallel to the plates is set to be 0.2555. The hard sphere model is assumed for gas particles, so that the relaxation time is given by setting $\omega = 0.5$ in (16). The Knudsen number $Kn = 0.1$ is considered.

The numerical results are listed in Fig. 4 and Fig. 5, where the temperature and normal stress profiles for M from 3 to 10 are presented. It is obvious that the temperature profile converges quickly as the number of moments increases, and the normal stress also converges, but not as fast as the temperature.

The same numerical example is investigated by Cai et al. (2012), while the model therein contains second order derivatives and is much more difficult to solve.

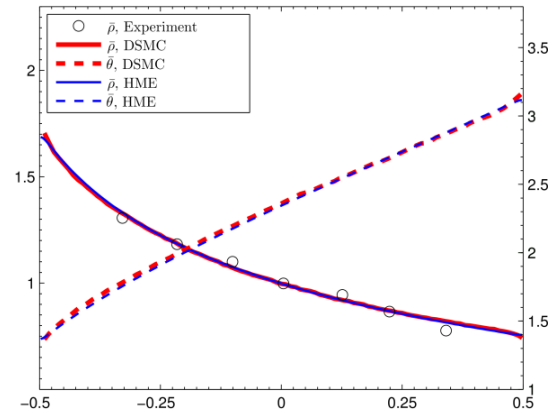


Fig. 1. Numerical results of heat transfer for $Kn=0.0658$.

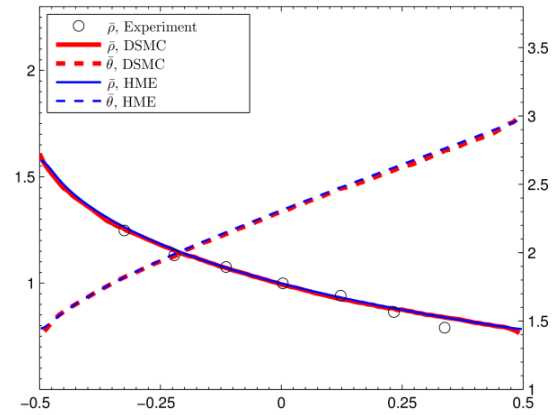


Fig. 2. Numerical results of heat transfer for $Kn=0.1044$.

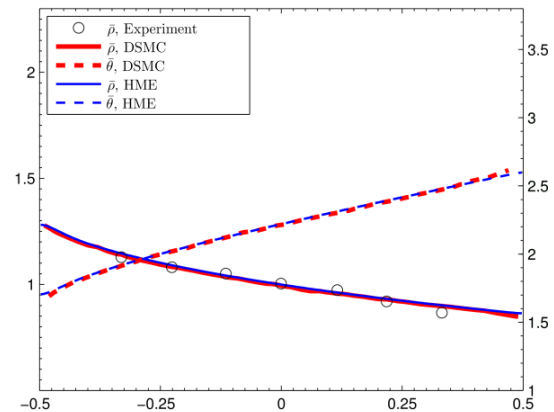


Fig. 3. Numerical results of heat transfer for $Kn=0.3521$.

7. Conclusion

This paper is an initial attempt to solve some problems in the field of microflows using the moment method. Both the models and the numerical methods presented in this paper are pretty new. The success in the

simulation of some simple processes encourages us to make more exploration in this direction. The moment models in this paper are still based on relatively simple Grad-type expansions, which are known to be inefficient in describing the Knudsen boundary layers. Improvement on the models is left for our future work.

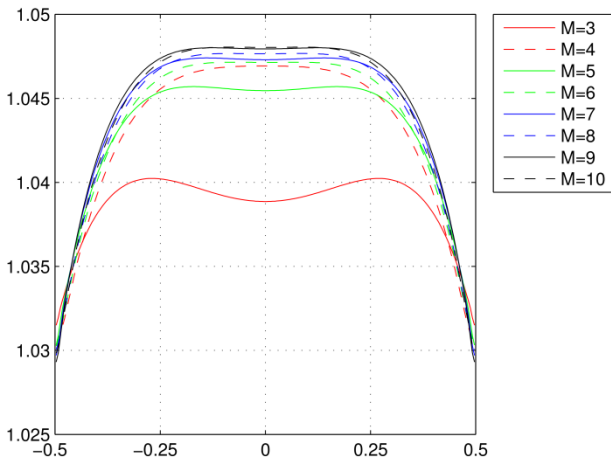


Fig. 4. Temperature profiles for the Poiseuille flow.

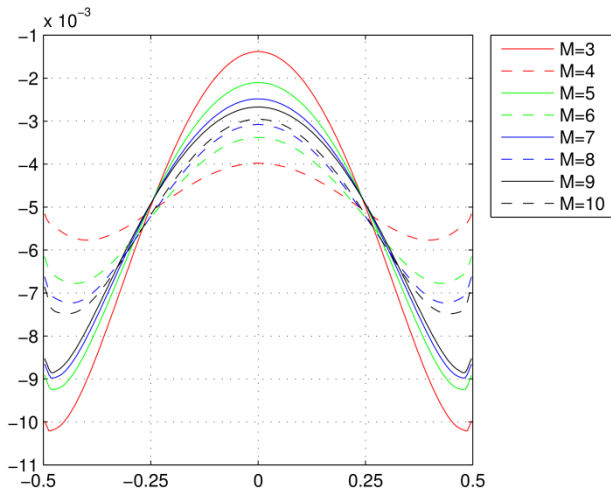


Fig. 5. Normal stress profiles for the Poiseuille flow.

References

Cai, Z., Fan, Y., Li, R., 2013a. Globally hyperbolic regularization of Grad's moment system in one dimensional space. *Commun. Math. Sci.* 11, 547-571.
 Cai, Z., Fan, Y., Li, R., 2014a. Globally hyperbolic regularization of Grad's moment system. *Commun. Pure Appl. Math.* 67, 464-518.
 Cai, Z., Fan, Y., Li, R., Qiao, Z., 2014b. Dimension-reduced hyperbolic moment method for the Boltzmann equation with BGK-type collision. *Commun. Comput. Phys.* 15,

1368-1406.
 Cai, Z., Li, R., 2010. Numerical regularized moment method of arbitrary order for Boltzmann-BGK equation. *SIAM J. Sci. Comput.* 32, 2875-2907.
 Cai, Z., Li, R., Qiao, Z., 2013b. Globally hyperbolic regularized moment method with applications to microflow simulation. *Computers Fluids* 81, 95-109.
 Cai, Z., Li, R., Qiao, Z., 2012. NRxx simulation of microflows with Shakhov model. *J. Sci. Comput.* 34, A399-A369.
 Grad, H., 1949. On the kinetic theory of rarefied gases. *Commun. Pure Appl. Math.* 2, 331-407.
 Gu, X., Emerson, D., 2007. A computational strategy for the regularized 13 moment equations with enhanced wall-boundary equations. *J. Comput. Phys.* 255, 263-283.
 Holway, L. H., 1966. New statistical models for kinetic theory: method of construction. *Phys. Fluids* 9, 1658-1673.
 Maxwell, J. C., 1878. On stresses in rarefied gases arising from inequalities of temperature. *Proc. R. Soc. Lond.* 27, 304-308.
 Rana, A., Torrilhon M., Struchtrup H., 2013. A robust numerical method for the R13 equations of rarefied gas dynamics: Application to lid driven cavity. *J. Comput. Phys.* 236, 169-186.
 Rhebergen, S., Bokhove, O., van der Vegt, J.J.W., 2008. Discontinuous Galerkin finite element methods for hyperbolic nonconservative partial differential equations. *J. Comput. Phys.* 227, 1887-1922.
 Struchtrup H., 2005. Derivation of 13 moment equations for rarefied gas flow to second order accuracy for arbitrary interaction potentials. *Multiscale Model. Simul.* 3, 221-243.
 Struchtrup H., Torrilhon M., 2003. Regularization of Grad's 13-moment equations: derivation and linear analysis. *Phys. Fluids* 15, 2668-2680.
 Torrilhon M., 2006. Two dimensional bulk microflow simulations based on regularized Grad's 13-moment equations. *Multiscale Model. Simul.* 5, 695-728.
 Torrilhon, M., 2014. Convergence study of moment approximations for boundary-value problems of the Boltzmann-BGK equation. Submitted.
 Wadsworth D. C., 1993. Slip effects in a confined rarefied gas. I: temperature slip. *Phys. Fluids* 5, 1831-1389.
 Zheng, Y., Alder, B. J., Garcia, A. L., 2002. Comparison of kinetic theory and hydrodynamics for Poiseuille flow. *J. Stat. Phys.*, 109, 495-505.